ORIGINAL ARTICLE

Metabolic plasticity of mixotrophic algae is key for their persistence in browning environments

Marco L. Calderini[1] | Pauliina Salmi[2] | Cyril Rigaud[1] | Elina Peltomaa[3,4] |
Sami J. Taipale[1]

[1]Department of Biological and Environmental Science, University of Jyväskylä, Jyväskylä, Finland

[2]Spectral Imaging Laboratory, Faculty of Information Technology, University of Jyväskylä, Jyväskylä, Finland

[3]Institute of Atmospheric and Earth System Research (INAR)/Forest Sciences, University of Helsinki, Helsinki, Finland

[4]Helsinki Institute of Sustainability Science (HELSUS), University of Helsinki, Helsinki, Finland

Correspondence
Marco L. Calderini, Department of Biological and Environmental Science, University of Jyvaskyla, Jyväskylä, Finland.
Email: marco.92.calderini@jyu.fi

Funding information
Academy of Finland, Grant/Award Number: 333564 and 321780

Handling Editor: Katie Lotterhos

Abstract

Light availability is the main regulator of primary production, shaping photosynthetic communities and their production of ecologically important biomolecules. In freshwater ecosystems, increasing dissolved organic carbon (DOC) concentrations, commonly known as browning, leads to lower light availability and the proliferation of mixotrophic phytoplankton. Here, a mixotrophic algal species (*Cryptomonas* sp.) was grown under five increasing DOC concentrations to uncover the plastic responses behind the success of mixotrophs in browning environments and their effect in the availability of nutritionally important biomolecules. In addition to the browning treatments, phototrophic, heterotrophic and mixotrophic growth conditions were used as controls. Despite reduced light availability, browning did not impair algal growth compared to phototrophic conditions. Comparative transcriptomics showed that genes related to photosynthesis were down-regulated, whereas phagotrophy gene categories (phagosome, lysosome and endocytosis) were up-regulated along the browning gradient. Stable isotope analysis of phospholipid fractions validated these results, highlighting that the studied mixotroph increases its reliance on heterotrophic processes with browning. Metabolic pathway reconstruction using transcriptomic data suggests that organic carbon is acquired through phagotrophy and used to provide energy in conjunction with photosynthesis. Although metabolic responses to browning were observed, essential fatty acid content was similar between treatments while sterol content was slightly higher upon browning. Together, our results provide a mechanistic model of how a mixotrophic alga responds to browning and how such responses affect the availability of nutritionally essential biomolecules for higher trophic levels.

KEYWORDS
browning, *Cryptomonas*, dissolved organic carbon, fatty acids, mixotrophy, phagotrophy, transcriptomic

1 | INTRODUCTION

Primary production is centrally important to ecological processes since it provides energy and essential biomolecules for upper trophic levels. Ultimately, harvesting of light energy depends on light availability and the ability of phototrophic organisms to regulate photosynthesis according to environmental cues (Gerbaud & André, 1980). When light becomes limiting, the capacity of a photosynthetic organism to utilize alternative sources of energy can manifest in a competitive advantage over obligate phototrophs. Mixotrophy refers to the capacity of organisms to complement their photosynthetic activity with exogenous organic carbon sources (i.e., uptake of sugars, engulfment of bacteria) to maintain or enhance their fitness. While such metabolic flexibility can be advantageous with transient low light, energetic and nutrient investments in light harvesting machinery are high (Raven, 1997). Consequently, mixotrophs present plastic responses to changes in light and organic carbon availability to maximize fitness (González-Olalla et al., 2021). Such changes can be ecologically relevant since they potentially affect the availability of nutritionally important biomolecules for higher trophic levels (Brett et al., 2006; Peltomaa et al., 2017).

In freshwater and costal ecosystems, increases in terrestrial dissolved organic carbon (DOC) loading is a process commonly called browning. The term browning refers to the darkening of water towards a brown colour which leads to reduced penetration of shorter wavelengths of the visible spectrum of solar radiation (Graneli, 2012). In lakes, this reduction in light availability has been linked to reduced dissolved oxygen concentrations (Couture et al., 2015), and reduced primary production (Thrane et al., 2014), as well as higher costs of drinking water purification (Hongve et al., 2004). Given that browning is associated with reduced acid deposition, increased precipitation and increased terrestrial primary production in catchment areas (Kritzberg et al., 2020), it is expected that climate change will further intensify ongoing brownification processes in surface waters (Björnerås et al., 2017; Kritzberg & Ekström, 2012; Spilling et al., 2022). In particular, the boreal zone could suffer more intense browning given the combination of increased precipitation (12%–20% expected increase; IPCC, 2013; Ruosteenoja et al., 2016) and the predominance of water bodies with peatland-dominated catchments. In addition to changes in water colour, mobilization of terrestrial DOC is accompanied by macronutrients such as nitrogen and phosphorus and micronutrients such as iron (Ged & Boyer, 2013; Maranger & Pullin, 2003; Qualls & Richardson, 2003). Together, these modifications in the physical and chemical properties of water are expected to disturb the balance between algal and bacterial production (Creed et al., 2018), reduce energy transfer efficiency through food webs (Hessen, 1998), and affect the availability of essential fatty acids (FAs) and sterols for consumers (Martin-Creuzburg et al., 2009; Parrish, 2009; Peltomaa et al., 2017; Sargent et al., 1995).

Phytoplankton communities observed in highly brown environments (high DOC concentration) are less diverse (Jones, 1992) and are usually dominated by mixotrophic flagellated species (Bergström et al., 2003; Deininger et al., 2017; Wilken et al., 2018).

Environmental data together with mesocosm studies have shown that mixotrophic cryptophytes, in particular the genus *Cryptomonas*, thrive in brown freshwater environments (Bergström et al., 2003; Deininger et al., 2017; Isaksson et al., 1999; Wilken et al., 2018), making them promising models of plastic and genetic adaptations to browning. Importantly, mesocosm studies suggest that mixotrophs respond to browning by enhancing bacterial predation (Wilken et al., 2018). Since bacteria make use of terrestrially derived DOC for growth (Kritzberg et al., 2006), and that active bacterial predation in mixotrophic algae has been linked to decreases in oxygen production (González-Olalla et al., 2021; Wilken et al., 2014), increasing algal mixotrophy with browning could alter the carbon and oxygen cycling of lakes. In addition, the trophic transition from phototrophic to mixotrophic, as well as variations in the physicochemical properties of water, can affect the FA and sterol content of algae (Boëchat et al., 2007; Peltomaa & Taipale, 2020; Piepho et al., 2010). Nevertheless, other responses to low light (i.e., changes in pigments), together with diel movements across the water column to avoid light limitation (Gervais, 1997), could also explain the success of mixotrophic flagellates in brown environments. Therefore, examining plastic responses of mixotrophic algae to browning is necessary to settle the bases for understanding the biogeochemistry, algal physiology and food web ecology of browning lakes.

In this study, we used *Cryptomonas* sp. (isolated from a clear water lake) as a model system for plastic responses to browning environments to ask the following questions: (i) is mixotroph growth negatively impacted by browning; (ii) does browning affect the use of light energy; (iii) does browning affect FA or sterol quality and quantity in mixotrophs; (iv) do mixotrophs change their photosynthetic pigment content with browning; and (v) which genes show differential expression between phototrophic, glucose-supplemented phototrophic and browning conditions? To answer these questions, we cultivated *Cryptomonas* sp. under three different control conditions (phototrophic, glucose-supplemented phototrophic and heterotrophic) in addition to five degrees of browning (DOC concentrations ranging from 1.5 to 90 mg C L^{-1}). During exponential growth, we performed a comparative transcriptome analysis followed by differential gene expression analysis between three browning treatments and two of our controls. The balance between phototrophic and heterotrophic activity was evaluated by the incorporation of ^{13}C-labelled carbon from $NaHCO_3$ into membrane lipids. At the end of the experiment, biomass analyses were carried out to observe differences in FAs, sterols and pigments between treatments.

2 | MATERIALS AND METHODS

2.1 | Strains, culture preparation and growing conditions

Cryptomonas sp. strain CPCC 336 was obtained from the Canadian Phycological Culture Centre, originally isolated from a clear-water lake, and thus was not readily adapted to brown waters. The algae

were maintained phototrophically in the authors' culture collection as stock cultures in MWC (Modified Wright's Cryptophyte) media (Guillard & Lorenzen, 1972) with some modifications (Stevčić et al., 2019; see Methods S1) at 18°C under light–dark cycle of 12:12 h (light intensity of 50–70 μmol quanta m^{-2} s^{-1}).

All experimental treatments described next were prepared in quadruplicate using our modified MWC media and grown using the same light conditions as the stock cultures. A photoautotrophic treatment (Control) was prepared using modified MWC media and *Cryptomonas* sp. inoculum. Two glucose-supplemented treatments (GLU and DARK) were prepared as Control and D-glucose (Sigma-Aldrich) was added to a final concentration of 5 mg C L^{-1}. One of these treatments was maintained in the dark during the course of the experiment (DARK treatment). Experimental DOC cultures (concentrations: 1.5, 10, 30, 50 and 90 mg C L^{-1}) were prepared using a DOC mix (500 mg C L^{-1}; see Methods S1), filtered lake water or a combination of both accounting for 18% of the culture's volume. The rest of the culture volume was MWC medium and the algae inoculum. All treatments were grown in 650-ml plastic culture flasks containing a final volume of 400 ml. To avoid carbon limitation, we weekly added 0.720 mg of carbon in the form of $NaHCO_3$ (to Control and DOC treatments) or glucose (to GLU and DARK) until the end of the experiment. All $NaHCO_3$ available in DOC treatments (initial MWC concentration and weekly additions) was enriched with 5% ^{13}C-$NaHCO_3$ (Sigma-Aldrich) for stable isotope analysis. Cell concentration was measured every 2–3 days using a flow cytometer (Guava easyCyte HT; Luminex).

2.2 | Bulk stable isotope analysis of phospholipid fraction

Cells were harvested on day 16 by filtration (50–100 ml of culture) through 3.0-μm cellulose nitrate membranes (Whatman, GE Healthcare), frozen at −80°C for 45 min, and freeze-dried overnight (three or four replicates). Total lipids were extracted with 3.75 ml chloroform/methanol/water (4:2:1) using sonication (10 min). After phase separation, solvents were evaporated at 50°C under a nitrogen stream, and 400 μl of chloroform was added to dried lipid samples. Phospholipid fractions of lipid extracts were obtained via solid-phase extraction using silica cartridges (500 mg, Bond Elut LRC—SI; Agilent). Cartridges were preconditioned with chloroform before the lipid extract was added. Chloroform and acetone (8 ml of each) were first used to elute nonpolar lipids, and the phospholipid fraction was eluted with 8 ml methanol. Chloroform fractions were stored at −20°C for sterol analysis. Phospholipids in methanol were dried at 50°C under a nitrogen stream, dissolved in methanol and added to a smooth-wall tin cup (D4057 Elemental Microanalysis). Tin cups were dried overnight under a fume hood, and the δ^{13}C values of these samples were analysed using a Thermo Finnigan DELTA^{plus}Advantage mass spectrometer (Thermo Electron) connected to a FlashEA 1112 Elementar Analyser. Birch leaves (*Betula pendula*) were used as internal standards during the run. In addition,

three replicates of freeze-dried DOC mix (500 mg C L^{-1}) were analysed to get their signature δ^{13}C value.

2.3 | Fatty acid and sterol analysis

Algal cells were harvested (2–5 mg dried weight) on day 16 and lipids extracted as described above. After phase separation and evaporation at 50°C, 500 μl of acetone was added, and 40% of the sample was stored for carotenoid analysis (−20°C). The rest of the sample was evaporated and dissolved in 1 ml toluene, and FAs were transesterified overnight (50°C) using methanolic H_2SO_4 (1%, v/v). FA methyl esters were analysed with a gas chromatograph equipped with a mass detector (GC–MS; Shimadzu Ultra) using a DB-23 column (30 m×0.25 mm×0.25 μm; Agilent). Quantification of FAs was based on peak integration using GCSOLUTION software (version 2.41.00, Shimadzu; see Methods S1). Peak areas of FAs were corrected by using two internal standards (phospholipid FA C19:0 and free FA C23:0; Larodan) added before lipid extraction. Replicates of DOC mix (500 mg C L^{-1}) were extracted and analysed for FAs as controls. Only FAs that were not identified or present in trace amounts in the DOC mix were used for comparisons between treatments (referred to as algal FAs in the text). For percentage calculations and FA content, only the algal ω-3 (18:3ω-3, 18:4ω-3, 20:4ω-3, 20:5ω-3 and 22:6ω-3) and ω-6 (18:2ω-6, 22:5ω-6) FAs were used.

Stored nonpolar lipid extracts for sterol analysis were evaporated at 50°C under a nitrogen stream. For silylation, 100 μl of pyridine (Sigma-Aldrich) and 70 μl of N,O-bis[trimethylsilyltrifluoroacetamide] (BSTFA) with 1% (w) trimethylchlorosilane (TMCS; Sigma-Aldrich) were added to all samples and incubated at 70°C overnight. Trimethylsilyl (TMS) derivatives of sterols were analysed with a gas chromatograph (GC-2010 Plus, Shimadzu) coupled to a flame ionization detector (FID-2010 Plus, Shimadzu) using a Phenomenex Zebron ZB-5 HT Inferno column (30 m×0.25 mm×0.25 μm) for separation (see Methods S1). Identification of sterols was based on retention times using a plant sterol mix (Larodan). Quantification was done using a three-point calibration curve based on known standard concentrations. Concentration corrections of sterol samples were done using the internal standard 5-α-cholestane (Sigma-Aldrich).

2.4 | Chlorophyll-*a* and carotenoids

Samples for chlorophyll-*a* concentration analysis were taken on day 16. Samples (2 ml of culture) were filtered with GF/C filters (Whatman) and stored at −20°C for less than 1 month before chlorophyll was extracted using hot 94% ethanol (wt%). Throughout the process, samples were handled in dim light and sheltered from direct light exposure. For extraction, filters were immersed in 10 ml ethanol and incubated at 75°C for 5 min. The obtained solution was filtered through 0.45-μm pore size nylon syringe filters (Whatman) into a 1-cm quartz cuvette. Absorbance at wavebands of 665 and 750 nm was measured with a Shimadzu UV-1800 spectrophotometer.

Chlorophyll-*a* was quantified utilizing an absorption factor of 11.9 (SFS-ISO 10260:1992).

Stored carotenoid samples (previously obtained aliquots of total lipids) were separated and analysed via ultrahigh-performance liquid chromatography (Nexera, Shimadzu) coupled with a SPD-M20A diode array detector (Shimadzu) using a YMC carotenoid column (250×4.6 mm.D. S-5 μm; YMC). Identification of carotenoids was done using retention times and absorption spectra of observed peaks. Quantification of carotenoids was achieved by using a previously obtained factor between the peak areas of the sample internal standard Trans-β-Apo-8′-carotenal (Sigma Aldrich) and the target carotenoid (see Methods S1).

2.5 | RNA preparation and transcriptomic analysis

After 14 days of cultivation, 50 ml of every culture was centrifuged for 5 min (2500 *g*, 18°C), after which the supernatant was discarded. Cell pellets were resuspended in 700 μl of DNA/RNA Shield and homogenized in BashingBead (0.1 and 0.5 mm) lysis tubes (Zymo Research) using a TerraLyzer Cell Disruptor. RNA was extracted using a Chemagic 360 and the Chemagic Viral DNA/RNA 300 Kit H96 following the manufacturer's instructions (PerkinElmer). Extracted RNA was treated with DNAse I (Thermo Fisher Scientific), purified using Zymo spin-columns and quantified using a NanoDrop (Thermo Fisher Scientific). Samples were stored at −80°C.

Control, DOC 1.5, DOC 30, DOC 90, and GLU treatments were selected for transcriptomic analysis. RNA library generation, transcriptome sequencing, and annotation and differential expression analysis of the chosen treatments were conducted by Novogene. Briefly, three biological replicates of each treatment were sequenced with a NovaSeq 6000 (Illumina) to produce 150-bp paired-end reads. The targeted number of reads for each sample was 30 million. After removing reads with adaptor contamination or uncertain nucleotides, de novo transcriptome assembly (in the absence of a reference genome) was carried out by TRINITY 2.6.6 (Grabherr et al., 2011). Clustering of contigs based on shared reads was done with CORSET 4.6 (Davidson & Oshlack, 2014) to remove transcriptome redundance. The completeness of the transcriptome was assessed by the Benchmarking Universal Single-Copy Orthologs (BUSCO 3.0.2; Simao et al., 2015) with the eukaryota odb9 database. Differential expression analysis (*p*-value estimation) was carried out using DESEQ2 (Love et al., 2014). DESEQ2 was used to normalize readcount data and a negative binomial distribution was used for *p*-value estimation model. The BH procedure was used as a false discovery rate estimation method. We selected a threshold of 2-fold change in expression between treatment and our phototrophic control (while having a significant *p*-value) to be considered a differentially expressed transcript (DET: $|\log_2 \text{FoldChange}| > 1$ and $p < .05$).

For transcript functional annotation, we matched the DETs = s to the Kyoto Encyclopedia of Genes and Genome (KEGG) Orthology (KO) database using KAAS (KEGG Automatic Annotation Server) with an evalue threshold of $1e^{-5}$. Given that many annotated genes

in the KO database had several matching DETs, we obtained the weighted average Log_2 fold-change expression change between treatments and Control for each KO gene ID. The weight of each transcript was assigned based on the transcript abundance value. To visualize changes in expression of genes involved in glycolysis, the tricarboxylic acid (TCA) cycle and photosynthesis, Figure 6 was prepared by manually selecting transcripts involved in these pathways. A Venn diagram of DETs was produced in R with the VENNDIAGRAM package (version 1.6.20).

2.6 | Statistics and stable isotope mixing model

Multiple comparisons were carried out with Dunnett's test comparing the results of Control against all other treatments. Before the analysis, homogeneity of variances was tested with Levene's test. Permutational multivariate analysis of variance (PERMANOVA) based on the Bray–Curtis distance matrix, as well as multivariate homogeneity of group dispersion (Anderson, 2006) were performed on FA, sterol and carotenoid contribution data (%) using treatment as the only factor. The limit of statistical significance in all tests was set to α = 0.05. All statistical analyses were conducted using R (RStudio version 3.6.3) with either R base or VEGAN package (Oksanen et al., 2018).

A two-source carbon isotope mixing model, ISOERROR, version 1.04 (Phillips & Gregg, 2001), was used to assess how much of the phospholipid-derived fatty acids (PLFAs) from DOC treatments originated from labelled inorganic carbon (phototrophic) and how much from DOC (heterotrophic). DOC 1.5 was selected as the most phototrophic of all DOC treatments due to its negligible light limitation, and hence used as the $\delta^{13}C$ value of highest phototrophy. The mean proportion of phototrophy PLFA (fA = labelled inorganic carbon) by our mixotrophic algae was calculated using the following mixing model:

$$(\text{fA}) = (\delta\text{M} - \delta\text{B}) / (\delta\text{A} - \delta\text{B})$$

where δM represents the $\delta^{13}C$ values of DOC treatments PLFA, δA represents the $\delta^{13}C$ value of DOC 1.5, and δB represents the $\delta^{13}C$ value of DOC mix. Isotopic fractionation was not considered since the variation of $\delta^{13}C$ values of PLFA and DOC mix varied more than previously measured isotopic fractionation (e.g., −4‰; Bec et al., 2011) due to the ^{13}C-enrichment.

3 | RESULTS

3.1 | Browning and cell growth

To assess the effects of browning on the studied mixotrophic algae, five naturally occurring DOC concentrations ranging from low to very high (1.5, 10, 30, 50 and 90 mg C L^{-1}; Figure S1) were studied and compared to fully phototrophic cultures (Control). In addition,

we examined the effects of glucose supplementation under phototrophic and heterotrophic conditions (GLU and DARK treatments, respectively). DARK treatment showed limited initial growth, and cell numbers started to decline after 2 days of cultivation. Therefore, this treatment was ended 2 days earlier than in the other cultures, and no further analyses were carried out. Glucose supplementation under phototrophic conditions enhanced growth, leading GLU to ~35% higher cell densities than Control and the overall highest cell densities of all treatments (Figure 1a). DOC concentrations from 1.5 to 50 mg C L^{-1} did not have a large impact on the growth curve, and these cultures reached similar final cell densities. DOC 90 had the highest cell densities of all DOC treatments, surpassing Control and achieving comparable, but overall lower, cell densities to GLU. The analysis of per day increase in cell population number, measured as specific growth rate, revealed that GLU (0.14 ± 0.004 day^{-1}), DOC 90 (0.13 ± 0.003 day^{-1}) and DOC 10 (0.12 ± 0.004 day^{-1}) treatments grew faster than Control (0.11 ± 0.001 day^{-1}; Dunnett's test, $p < .05$), while no statistically significant differences were seen between the other cultures and Control (Figure 1b). In summary, our results with glucose supplementation show that our model algae cannot grow heterotrophically, but mixotrophic conditions enhance growth. In addition, since browning reduces the amount of available photosynthetically active light, our results from DOC treatments suggest a mechanism to bypass this reduction in light to sustain and even potentiate growth.

3.2 | Nutritionally important biomolecules

In view of the ecological importance of the nutritional quality of algae for higher trophic levels, we tested if browning leads to an alteration in the composition or concentration of FAs and sterols. Overall, 22 FAs and three sterols were identified and quantified. Because bacteria and the organic matter present in the DOC mixture used to prepare our DOC treatments contained FAs (see DOC extract preparation, Methods S1), we selected seven nutritionally important algal ω-3 and ω-6 FAs that were not present in the DOC mixture. The contribution of linolenic acid (LIN, 18:2ω-6), alpha-linolenic acid (ALA, 18:3ω-3), stearidonic acid (SDA, 18:4ω-3), 20:4ω-3, eicosapentaenoic acid (EPA, 20:5 ω-3), 22:5ω-6, and docosahexaenoic acid (DHA, 22:6 ω-3) to total algal FAs was affected by treatment. Of the total variance observed, 68% was explained by the factor treatment ($p < .05$, PERMANOVA; Figure 2a; Tables S1 and S2). Nevertheless, total ω-3 and ω-6 FA cell contents were not significantly different between Control (5.32 ± 0.95 and 0.40 ± 0.06 pg per cell ω-3 and ω-6, respectively) and the rest of the treatments (Figure 2b,c).

Sterol composition and content showed a strong response to browning. Brassicasterol and stigmasterol were found in all treatments, but beta-sitosterol was only observable in the browning treatments (Figure 2d) and was highest for DOC 30 (7.4% of all sterols). Sterol concentration data showed that all DOC treatments had slightly higher total sterol concentrations than Control (0.44 ± 0.07 pg per cell). DOC 10 (0.92 ± 0.15 pg per cell), DOC 30 (0.97 ± 0.15 pg per cell) and DOC 90 (0.95 ± 0.38 pg per cell) had significantly higher total sterol concentrations (Figure 2e).

3.3 | Utilization of inorganic carbon

Since enhanced mixotrophy can increase the reliance of algae on organic carbon for growth, we tested if browning produces a change in the utilization of inorganic carbon. For this, we used isotopically
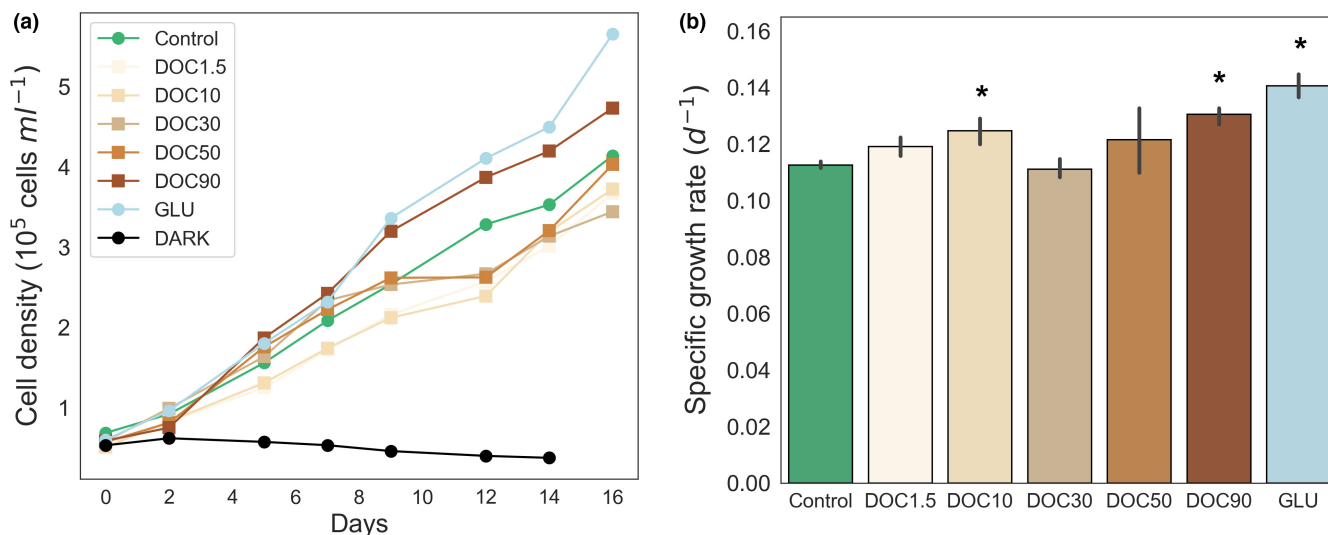

FIGURE 1 Cell growth under increasing DOC concentration and glucose supplementation. Cell density dynamics (a) and specific growth rate (b) of our mixotrophic algae model (*Cryptomonas* sp.) grown under phototrophic (control), glucose-supplemented phototrophic (GLU) or heterotrophic (DARK) conditions and under experimental concentrations of DOC. DOC concentrations ranged from 1.5 to 90 mg C L^{-1}. Values are presented as mean ± SD of three to four replicates. Statistically significant differences between one of the treatments and control are shown with an asterisk (Dunnett's test).
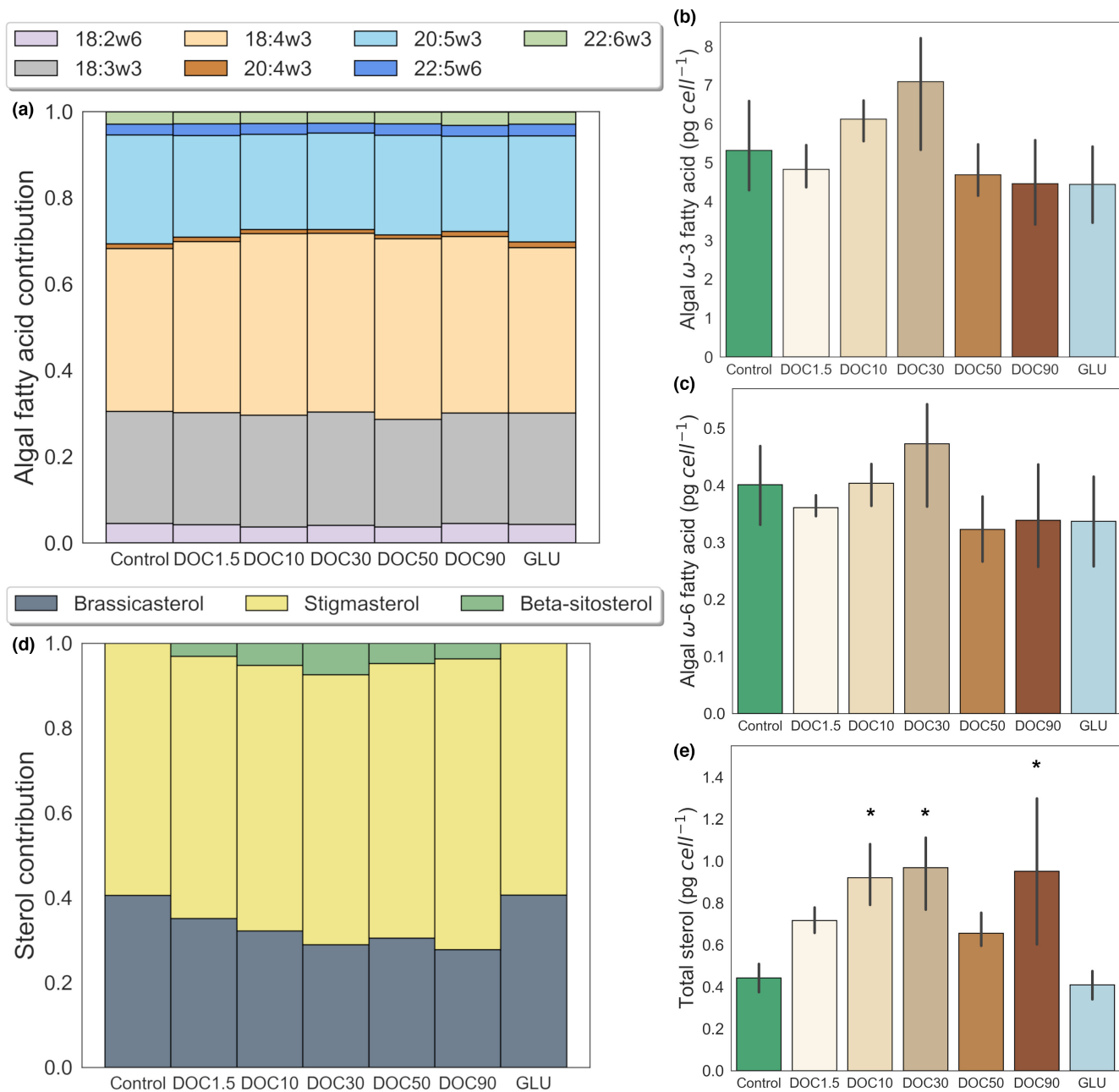
FIGURE 2 Changes in ecologically important biomolecules among DOC concentration increases or glucose supplementation (GLU). Algal fatty acid (a) and sterol (d) contribution to individual species of these groups of biomolecules. Total algal ω-3 and ω-6 fatty acid (b and c respectively) and sterol (e) content were normalized per cell. DOC concentrations ranged from 1.5 to 90 mg C L^{-1}. Values are presented as mean ± SD of three to four replicates for (a)–(c), while only the mean is given in contribution plots.

^{13}C-labelled sodium bicarbonate (^{13}C-NaHCO$_3$) in all browning treatments and followed its incorporation into the algal phospholipidic fraction. Phospholipids were used instead of total lipids, since phospholipids are rapidly degraded upon cell death and are therefore representative of viable biomass (Pinkart et al., 2002). Increases in the degree of browning led to a reduction in the incorporation of heavier carbon into phospholipids (Figure 3a). DOC 1.5 had the highest incorporation of ^{13}C (134.5 ± 7.1 δ^{13}C), whereas DOC 90 had the lowest (75.4 ± 8.1 δ^{13}C). Mixing model results using DOC 1.5 as

the baseline for phototrophy (100% reliance on inorganic carbon) showed that increases in DOC were associated with increases in heterotrophy (Figure 3b). Accordingly, the lowest inorganic carbon incorporation was seen in DOC 90 (63 ± 2.9% of carbon use; Figure 3b). These results suggest that there is a rapid switch in the utilization of carbon from inorganic to organic sources with browning. Therefore, given the similar growth rates obtained for DOC treatments, mixotrophs may reduce their dependence on phototrophy to sustain growth.
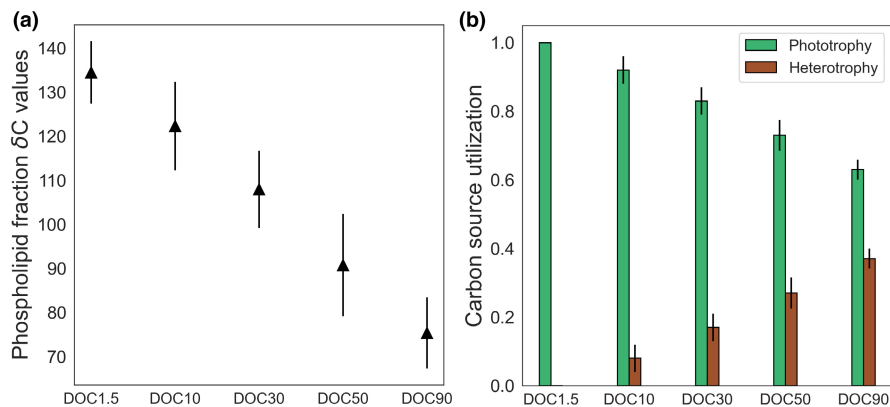
FIGURE 3 Utilization of inorganic (phototrophy) and organic (heterotrophy) carbon among changes in DOC concentration. Phospholipid fraction δC values (a) of 5% ^{13}C-NaHCO$_3$-enriched DOC treatments among increasing DOC concentrations. Mixing model results of carbon source utilization (b) using DOC 1.5 as the most phototrophic of all DOC treatments (see Section 2). Values are presented as mean±SD of three to four replicates.
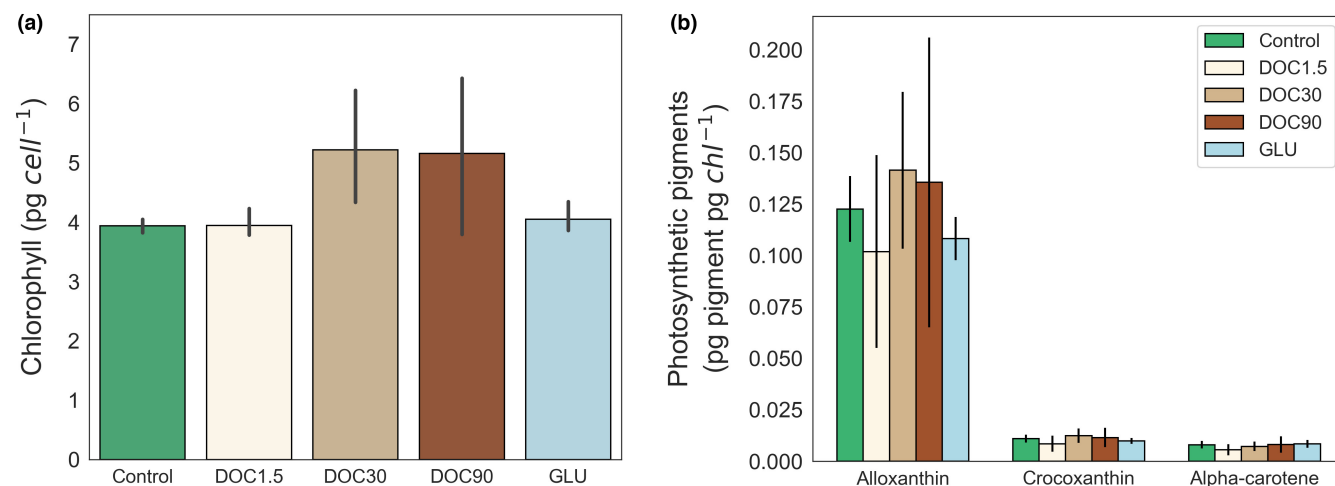
FIGURE 4 Pigment variation in response to increases in DOC concentration and glucose supplementation (GLU). Total chlorophyll-*a* normalized per cell (a) and carotenoid content relative to chlorophyll-*a* (b) of three DOC treatments and GLU compared to phototrophic conditions (control). Values are presented as mean (±SD in a and c) of three to four replicates. Statistically significant differences between one of the treatments and control are shown with an asterisk (Dunnett's test).

3.4 | Chlorophyll and carotenoids

Since manipulation of photosynthetic pigments can increase light energy harvesting under reduced light availability, we then investigated the chlorophyll-*a* and carotenoid content per cell of Control, GLU and three of the DOC treatments (1.5, 30 and 90 mg C L^{-1}). Chlorophyll-*a* concentration per cell was not affected by browning or glucose supplementation compared to Control (3.94 ± 0.09 pg per cell), despite slightly higher average contents in DOC 30 and DOC 90 (Figure 4a). Alloxanthin, crocoxanthin and alpha-carotene were the three identified carotenoids in all samples (Figure 4b). Alloxanthin was the highest contributing carotenoid (>80%) of all quantified carotenoids, followed by crocoxanthin (~8%) and alpha-carotene (~5%). The contribution of individual carotenoids did not vary between treatments ($p > .05$, PERMANOVA; Table S1). Carotenoid content relative to chlorophyll-*a* was not affected by browning or glucose supplementation (Figure 4b). As expected, alloxanthin relative to chlorophyll-*a* content was the highest of all carotenoids (0.151 ± 0.05 pg pg^{-1} in Control), highlighting this carotenoid as the main light-harvesting accessory pigment.

3.5 | Transcriptomic analysis

To gain insight into genome-wide gene expression changes that modulate the adaptation of mixotrophs to browning, we conducted a de novo RNA sequencing (RNA-seq) analysis of five of our treatments (Control, DOC 1.5, DO 10, DOC 90 and GLU). More than 30 million raw reads were obtained per sample and the final transcript length varied from 301 to 40,155 nucleotides with a mean length of 1266 nucleotides (Tables S3 and S4). Transcriptome assembly identified ~250,000 unique transcripts (Table S4). The ompleteness of the assembled transcriptome was low in BUSCO (79.4% missing; Table S5). Nevertheless, these results were not surprising given the evolutionary divergence of cryptophytes and the fact that many of the genes in the Eukaryotic database are absent in many highly contiguous algal genomes (Curtis et al., 2012; Hanschen et al., 2020). No genomic data are currently available for *Cryptomonas* sp., but the related cryptophyte *Guillardia theta* showed the highest species similarity (49.3%) based on transcriptome species classification (Figure S2). Functional annotation of the assembled transcriptome exhibited a large number of novel transcripts that did not match with

any sequence in available databases (51.1% of the transcriptome). To examine the effects of browning and glucose supplementation on gene expression, we identified all DETs between these treatments and Control. Transcripts were only considered differentially expressed if the change in transcript abundance between treatment and Control was 2-fold or more in either direction while having a significant p-value (DET: $|log_2FoldChange| > 1$ and $p < .05$).

Close to a fifth of all transcripts in the transcriptome were differentially expressed upon browning or glucose supplementation (51,427 out of 254,822 total transcripts; Figure 5). Increases in the degree of browning had a strong effect on gene expression, with an almost 2-fold increase in the number of DETs between DOC 1.5 and DOC 30 (8273 and 17,585 transcripts, respectively) and DOC 30 and DOC 90 (17,585 and 30,187 transcripts, respectively; Figure 5a). In comparison, glucose supplementation led to a change in the expression of 10,358 transcripts. All treatments shared >1200 DETs while >500 transcripts were differentially expressed in DOC treatments alone (Figure 5b). Overall, more than 55% of each treatment's DETs were up-regulated, and DOC 90 presented the highest percentage of up-regulated transcripts (>75% of all DETs).

For further analysis, we carried out a functional enrichment analysis using the KO database. Since we did not have a genomic sequence to map the assembled transcriptome against, many annotated genes in the KO database presented several matching transcripts. Therefore, to obtain the expression levels of individual genes, we used the weighted average log_2 fold-change expression with respect to Control of all identified transcripts matching one KO identifier. Given our previous results showing changes in inorganic carbon utilization along the DOC gradient, we focused on transcriptomic evidence of changes in metabolic pathways related to phagocytosis, light energy conversion and respiration. KO classifications (gene groups) specific to phagotrophic activity (phagosome, lysosome and endocytosis) had a higher number of up-regulated compared to down-regulated genes in all DOC treatments (Figure 5c).

Moreover, the number of up-regulated differentially expressed genes (DEGs) involved in phagotrophic activity increased along the browning gradient from 41 to 72 with an average log_2 fold-change increase of 4.49 9.64 in DOC 1.5 to DOC 90, respectively. In contrast, GLU had a higher number of down- than up-regulated DEGs in the same KO classifications (eight up- and 14 down-regulated genes) and an average log_2 fold-change of −0.37. These results suggest that browning, but not glucose supplementation, stimulates phagotrophic activity.

We then mapped RNA abundance changes upon DOC increases and glucose supplementation to metabolic genes involved in glycolysis, the TCA cycle and photosynthesis (Figure 6). Photosynthetic

FIGURE 5 Transcriptome responses to increases in DOC concentrations and glucose supplementation (GLU). Differentially expressed transcripts (a) were considered all transcripts that were more than 2-fold up- or down-regulated relative to the phototrophic control (control) samples having a $p < .05$ (see Section 2). Venn diagram (b) showing the overlap of differentially expressed transcripts (up- and down-regulated) between DOC and GLU treatments. DEGs in phagotrophy-related gene categories (phagosome, endocytosis and lysosome; c) represent phagotrophic activity among increases in DOC or glucose supplementation. Functional annotation of transcripts into phagotrophy-related gene categories was done using the KO database (Data Set S1). To obtain the number of unique genes in each category, weighted averages of all differentially expressed transcripts between each treatment and control matching the same gene ID in the KO database were used. Data represent the means of three biological replicates.
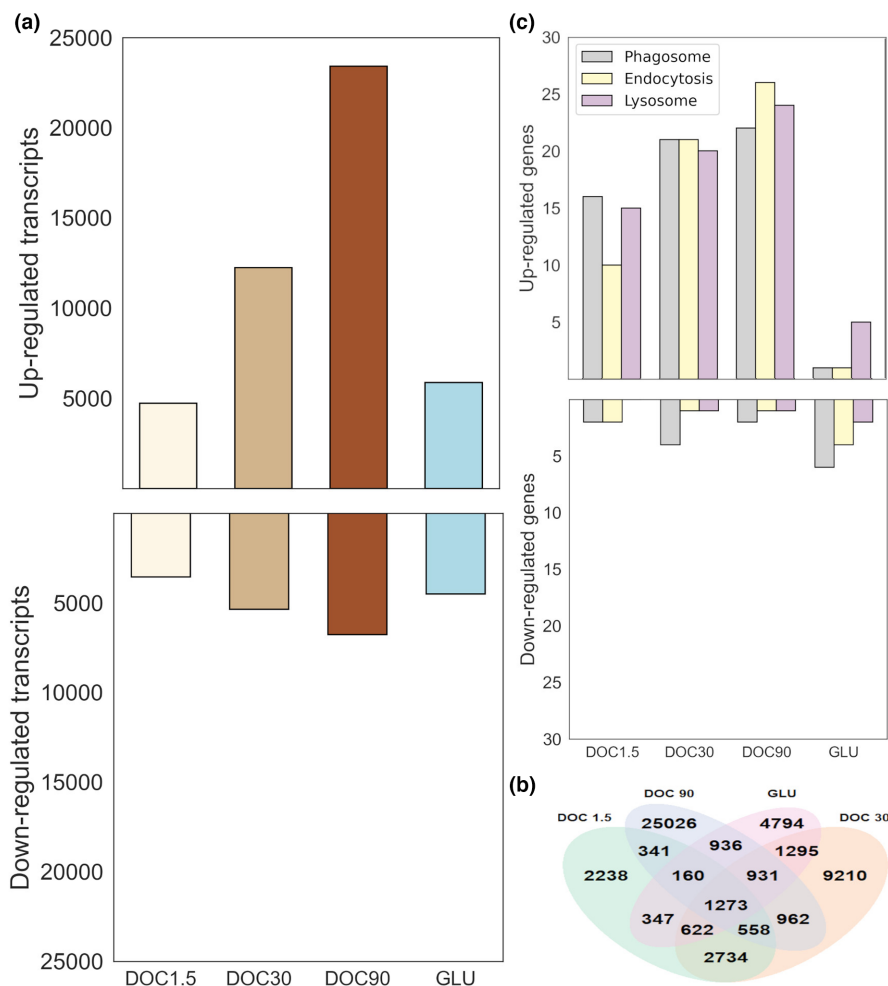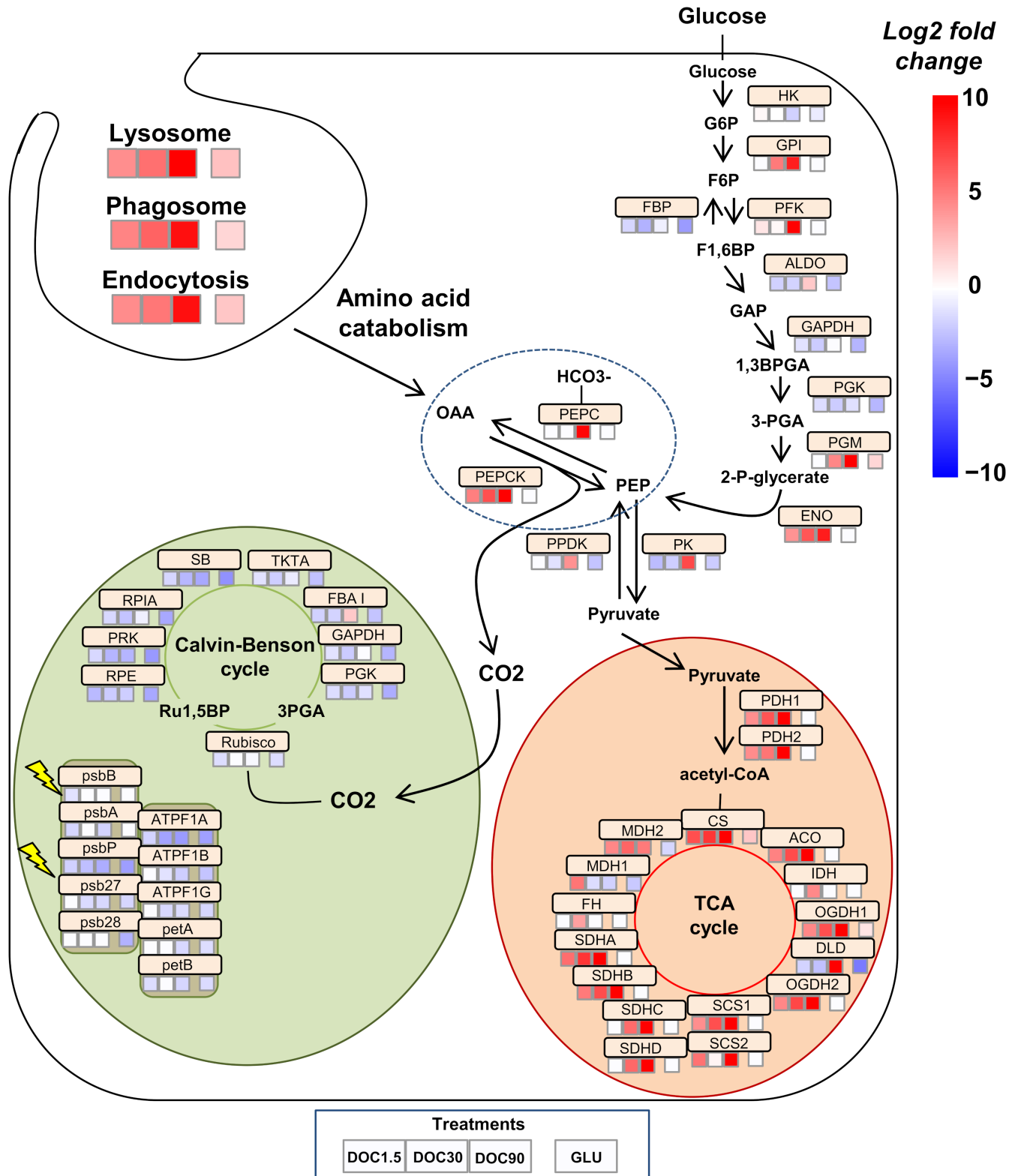
FIGURE 6 Adaptations in photosynthesis, glycolysis and TAC cycle among increases in DOC concentration and glucose supplementation (GLU). Functional annotation of genes was done with the KO database. Squares beneath gene names represent Log_2 fold-change values of the respective treatment and the phototrophic control. Log_2 fold-change values were obtained with the weighted average of all transcripts matching the same KO gene ID. Under gene groups, lysosome, phagosome and endocytosis, squares represent the average Log_2 fold-change value of all up-regulated genes in that category. Plastid is indicated in green, mitochondrion in red and cytosol in white. Data represent the means of three biological replicates. Fold-change values and gene IDs are in Data Set S2.

transcripts (enzymes of the Calvin–Benson cycle and electron transport chain complexes) were down-regulated in DOC and GLU treatments compared to Control. Interestingly, only photosystem II (PSII) components, proton-translocating ATPase, cytochrome b6f and ferredoxin were down-regulated, while no gene matching to photosystem I was differentially expressed between treatments. TCA cycle enzyme transcripts were highly up-regulated in all DOC treatments, while glucose supplementation did not affect their expression compared to the Control. Transcript abundance of glycolytic enzymes presented an overall increase along the browning gradient, although no general pattern of up- or down-regulation of the complete pathway was seen.

Similarly to TCA cycle genes, glucose supplementation did not produce significant expression changes in glycolytic enzymes. The two phosphoenolpyruvate (PEP) enzymes suggested to play a critical role in bacterial ingestion by mixotrophs (González-Olalla et al., 2021; Liu et al., 2016), carboxykinase (PEPCK) and carboxylase (PEPC), had contrasting expression patterns among treatments. PEPCK was up-regulated in all DOC treatments compared to Control, and its transcript abundance was increased along the browning gradient. In contrast, PEPC was only up-regulated in DOC 90, and no change in expression was found in the other two DOC treatments. Expression of none of these enzymes was affected by glucose supplementation compared to Control. In summary, our transcriptomic results indicate apparent differences in carbon metabolism upon browning and glucose supplementation and support our previous results on the decreasing reliance on phototrophy with browning.

4 | DISCUSSION

The impact of browning processes in aquatic ecosystems includes a shift from autotrophic to heterotrophic-based basal production (Creed et al., 2018). This study provides physiological, biochemical and transcriptomic evidence supporting such a prediction, indicating that browning leads to an increased reliance on heterotrophically acquired energy in our model mixotroph (*Cryptomonas* sp.). Our growth rate results validated using the selected algae species as a model mixotroph since glucose supplementation in the presence of light enhanced growth, as previously seen with other mixotrophic species (Smith et al., 2015; Zhang et al., 2021). In addition, fully heterotrophic conditions could not sustain growth, highlighting the need for basal levels of phototrophy for survival. Increases in water colour, and its associated reduction in light availability (Graneli, 2012), did not impair growth compared to fully phototrophic conditions. Conversely, two of our browning treatments (DOC 10 and DOC 90) had higher specific growth rates than under purely phototrophic conditions. Nevertheless, since increases in growth rate were modest with browning, we do not believe that such differences alone explain the dominance of mixotrophic flagellates observed in highly brown environments (Bergström et al., 2003; Deininger et al., 2017).

Given that increases in water colour did not negatively impact growth, we investigated if inorganic carbon fixation is altered by browning in the studied mixotrophic algae. Our stable isotope analysis of phospholipid fractions showed that increases in water colour come with a reduction in inorganic carbon utilization for growth. Furthermore, as demonstrated by our transcriptomic results, the down-regulation of genes related to photosynthesis further supports this claim and indicates a decreased reliance on phototrophy with browning. Notably, even our lowest DOC concentration (DOC 1.5) showed a down-regulation of photosynthetic genes. These results suggest that when organic carbon is available, mixotrophs may rapidly capitalize on their ability to increase reliance on heterotrophy to sustain growth, possibly to decrease the high energetic costs of maintaining photosynthetic machinery (Raven, 1995). Such changes in the balance between phototrophy and heterotrophy with browning could potentially impact oxygen production and carbon cycling in mixotrophic-dominated environments. Nevertheless, further studies are needed to observe how oxygen production is affected by increases in water colour.

Surprisingly, despite a reduction of phototrophy with browning, we did not observe a decrease in the chlorophyll or carotenoid content per cell. Previous studies on plastic responses of chlorophyll levels to mixotrophy suggest that, together with the down-regulation of photosynthesis, there is a reduction in the production or enhanced degradation of chlorophyll (González-Olalla et al., 2021; Roth et al., 2019; Wilken et al., 2014). Nevertheless, these studies were carried out using algae species that can grow fully heterotrophically; hence, our model mixotroph (which requires light to survive) might have specific needs to maintain basal photosynthetic function.

Enhanced expression of genes associated with phagotrophy (lysosome, endosome and phagosome KO categories) with browning, but not with glucose supplementation, suggests that heterotrophy was supported by predation of bacteria. These results agree with mesocosm experiments by Wilken et al. (2018), where mixotrophs showed higher bacterial predation along with temperature and water colour increases. Although the phagotrophy-related genes used in our analysis have been identified in macrophages and could have different functions in algae (Bohdanowicz & Grinstein, 2013; Flannagan et al., 2012; Settembre et al., 2013), other laboratory studies have observed expression of these groups of genes in algae growing under mixotrophic conditions (Li et al., 2021; Lie et al., 2017; McKie-Krisberg et al., 2018). In addition, the high expressions observed for key phagotrophy enzymes (PEPCK and PEPC) in our browning treatments agree with previous studies on phagotrophic activity of algae (González-Olalla et al., 2021; Liu et al., 2016; McKie-Krisberg et al., 2018). PEPCK is believed to be the enzyme by which degraded bacterial proteins are channelled to energy production (González-Olalla et al., 2021; Liu et al., 2016). Following this, oxidation of organic substrates has been shown to accelerate in the presence of bacterial prey (González-Olalla et al., 2021), which matches the up-regulation of the TCA cycle genes observed in our experiment with browning.

The availability and quality of FAs and sterols in phytoplankton have been repeatedly demonstrated as necessary for the growth and reproduction of zooplankton (Brett & Müller-Navarra, 1997;

Martin-Creuzburg et al., 2009; Peltomaa et al., 2017). This has great ecological importance since zooplankton have a key position in aquatic food webs, linking the flow of dietary energy and essential biomolecules from phytoplankton to fish (Taipale et al., 2016). The FA concentration remained unaffected in our experiment while the sterol content and composition varied between browning and fully phototrophic conditions. Since the switch from phototrophy to heterotrophy has been previously characterized by plastic changes in both FAs and sterols in algae (Boëchat et al., 2007), it is possible that particular FAs and sterols are required for structural adaptations that occur during these transitions. We hypothesize that the higher phagotrophic activity associated with browning could potentially explain the differences in composition and content observed in sterols. We can only speculate that sterol requirements for our glucose-supplemented treatment were not different from fully phototrophic conditions, explaining why there were no differences between these treatments. Our results suggest that browning in mixotroph-dominated environments should not reduce the availability of ecologically important biomolecules at a cellular level. Nevertheless, further studies with other mixotrophic species are needed to observe if the regulatory strategies seen in *Cryptomonas* sp. with browning are common or diversified among mixotrophs.

Overall, we report the metabolic plastic changes, and the possible ecological implications, behind the success of a model mixotroph in browning environments. As observed in our study, metabolic plasticity allows *Cryptomonas* sp. to thrive in low light environments, where obligated phototrophs are limited by photosynthetic output. Furthermore, we showed that an enhanced reliance on bacterial prey accompanies the transition to mixotrophic growth; hence, the consequences of such a shift in aquatic ecosystems could signify higher CO_2 exportations but increased reliance of whole food webs on bacterial production. Further studies could look more directly into the biogeochemical consequences of phototrophy to mixotrophy transitions. In addition, since we studied the plastic adaptations of a mixotroph isolated from a clear-water lake, investigating the differences between evolved and plastic effects of browning is important in understanding the genetic architecture necessary for algae to thrive in browning environments.

AUTHOR CONTRIBUTION

M.L.C., P.S., E.P. and S.J.T. planned and designed the research. M.L.C., P.S. and C.R. performed the analysis. M.L.C. analysed the data. M.L.C., P.S., E.P. and S.J.T. interpreted the data. M.L.C. wrote the manuscript in collaboration with P.S., E.P., C.R. and S.J.T.

ACKNOWLEDGEMENTS

CONFLICT OF INTEREST

The authors declare no conflict of interest.

DATA AVAILABILITY STATEMENT

Raw transcriptomic sequence reads, as well as processed transcriptomic data, are available in the ArrayExpress database (http://www.ebi.ac.uk/arrayexpress) under accession no. "E-MTAB-11370." Raw phenotypic data and the mixing model used are available in the Data Set S3. All data as exportable files and data analysis files necessary to replicate the results presented in this study are available at https://doi.org/10.17011/jyx/dataset/80823. A comprehensive description of the content of each file, and the description of each Supporting Information data set can be found in the same DOI under the name "Metadata file."

ORCID

Marco L. Calderini 🟢 https://orcid.org/0000-0003-2532-3167

REFERENCES

Anderson, M. J. (2006). Distance-based tests for homogeneity of multivariate dispersions. *Biometrics*, *62*, 245–253.

Bec, A., Perga, M., Koussoroplis, A., Bardoux, G., Desvilettes, C., Bourdier, G., & Mariotti, A. (2011). Assessing the reliability of fatty acid–specific stable isotope analysis for trophic studies. *Methods in Ecology and Evolution*, *2*, 651–659.

Bergström, A. K., Jansson, M., Drakare, S., & Blomqvist, P. (2003). Occurrence of mixotrophic flagellates in relation to bacterioplankton production, light regime and availability of inorganic nutrients in unproductive lakes with differing humic contents. *Freshwater Biology*, *48*, 868–877.

Björnerås, C., Weyhenmeyer, G. A., Evans, C. D., Gessner, M. O., Grossart, H., Kangur, K., Kokorite, I., Kortelainen, P., Laudon, H., Lehtoranta, J., Lottig, N., Monteith, D. T., Nõges, P., Nõges, T., Oulehle, F., Riise, G., Rusak, J. A., Räike, A., Sire, J., ... Kritzberg, E. S. (2017). Widespread increases in iron concentration in European and north American freshwaters. *Global Biogeochemical Cycles*, *31*, 1488–1500.

Boëchat, I., Weithoff, G., Krüger, A., Gücker, B., & Adrian, R. (2007). A biochemical explanation for the success of mixotrophy in the flagellate *Ochromonas* sp. *Limnology and Oceanography*, *52*, 1624–1632.

Bohdanowicz, M., & Grinstein, S. (2013). Role of phospholipids in endocytosis, phagocytosis, and macropinocytosis. *Physiological Reviews*, *93*, 69–106.

Brett, M., & Müller-Navarra, D. (1997). The role of highly unsaturated fatty acids in aquatic foodweb processes. *Freshwater Biology*, *38*, 483–499.

Brett, M., Müller-Navarra, D., Ballantyne, A., Ravet, J., & Goldman, C. (2006). Daphnia fatty acid composition reflects that of their diet. *Limnology and Oceanography.*, *51*(5), 2428–2437.

Couture, R. M., De Wit, H. A., Tominaga, K., Kiuri, P., & Markelov, I. (2015). Oxygen dynamics in a boreal lake responds to long-term changes in climate, ice phenology, and DOC inputs. *Journal of Geophysical Research: Biogeosciences*, *120*, 2441–2456.

Creed, I. F., Bergström, A. K., Trick, C. G., Grimm, N. B., Hessen, D. O., Karlsson, J., Kidd, K. A., Kritzberg, E., McKnight, D. M., Freeman, E. C., Senar, O. E., Andersson, A., Ask, J., Berggren, M., Cherif, M., Giesler, R., Hotchkiss, E. R., Kortelainen, P., Palta, M. M., ... Weyhenmeyer, G. A. (2018). Global change-driven effects on

dissolved organic matter composition: Implications for food webs of northern lakes. *Global Change Biology*, 24, 3692–3714.

Curtis, B., Tanifuji, G., Burki, F., Gruber, A., Irimia, M., Maruyama, S., Arias, M. C., Ball, S. G., Gile, G. H., Hirakawa, Y., Hopkins, J. F., Kuo, A., Rensing, S. A., Schmutz, J., Symeonidi, A., Elias, M., Eveleigh, R. J. M., Herman, E. K., Klute, M. J., … Archibald, J. M. (2012). Algal genomes reveal evolutionary mosaicism and the fate of nucleomorphs. *Nature*, 492, 59–65.

Davidson, N. M., & Oshlack, A. (2014). Corset: Enabling differential gene expression analysis for de novoassembled transcriptomes. *Genome Biology*, 15, 410.

Deininger, A., Faithfull, C. L., & Bergström, A. K. (2017). Phytoplankton response to whole lake inorganic N fertilization along a gradient in dissolved organic carbon. *Ecology*, 98, 982–994.

Flannagan, R. S., Jaumouillé, V., & Grinstein, S. (2012). The cell biology of phagocytosis. *Annual Review of Pathology: Mechanisms of Disease*, 7, 61–98.

Ged, E. C., & Boyer, T. H. (2013). Molecular weight distribution of phosphorus fraction of aquatic dissolved organic matter. *Chemosphere*, 91, 921–927.

Gerbaud, A., & André, M. (1980). Effect of CO_2, O_2, and light on photosynthesis and photorespiration in wheat. *Plant Physiology*, 66(6), 1032–1036.

Gervais, F. (1997). Diel vertical migration of cryptomonas and chromatium in the deep chlorophyll maximum of a eutrophic lake. *Journal of Plankton Research*, 19(5), 533–550.

González-Olalla, J. M., Medina-Sánchez, J. M., Norici, A., & Carrillo, P. (2021). Regulation of phagotrophy by prey, low nutrients, and low light in the mixotrophic haptophyte *Isochrysis galbana*. *Microbial Ecology*, 82, 981–993.

Grabherr, M. G., Haas, B. J., Yassour, M., Levin, J., Thompson, D., Amit, I., Adiconis, X., Fan, L., Raychowdhury, R., Zeng, Q., Chen, Z., Mauceli, E., Hacohen, N., Gnirke, A., Rhind, N., di Palma, F., Birren, B. W., Nusbaum, C., Lindblad-Toh, K., … Regev, A. (2011). Full-length transcriptome assembly from RNA-seq data without a reference genome. *Nature Biotechnology*, 29, 644–652.

Graneli, W. (2012). Brownification of lakes. In L. Bengtsson, H. LW, & R. W. Fairbridge (Eds.), *Encyclopedia of lakes and reservoirs* (pp. 117–119). Springer.

Guillard, R. R. L., & Lorenzen, C. J. (1972). Yellow-green algae with chlorophyllide C. *Journal of Phycology*, 8, 10–14.

Hanschen, E., Hovde, B., & Starkenburg, S. (2020). An evaluation of methodology to determine algal genome completeness. *Algal Research*, 51, 102019.

Hessen, D. O. (1998). Food webs and carbon cycling in humic lakes. In L. J. Tranvik & D. O. Hessen (Eds.), *Aquatic humic substances: Ecologyand biochemistry* (pp. 285–315). Springer-Verlag.

Hongve, D., Riise, G., & Kristiansen, J. F. (2004). Increased colour and organic acid concentrations in Norwegian forest lakes and drinking water—A result of increased precipitation? *Aquatic Sciences*, 66, 231–238.

IPCC (2013). Summary for policymakers. In T. F. Stocker, D. Qin, G.-K. Plattner, M. Tignor, S. K. Allen, J. Boschung, A. Nauels, Y. Xia, V. Bex, & P. M. Midgley (Eds.), *IPCC. 2013. Climate Change 2013: The physical science basis. Contribution of working group I to the fifth assessment report of the intergovernmental panel on climate change* (pp. 3–29). Cambridge University Press.

Isaksson, A., Bergstrom, A. K., Blomqvist, P., & Jansson, M. (1999). Bacterial grazing by phagotrophic phytoflagellatesin a deep humic lake in northern Sweden. *Journal of Plankton Research*, 21, 247–268.

Jones, R. I. (1992). The influence of humic substances on lacustrine planktonic food-chains. *Hydrobiologia*, 229, 73–91.

Kritzberg, E., Langenheder, S., & Lindström, E. (2006). Influence of dissolved organic matter source on lake bacterioplankton structure and function–implications for seasonal dynamics of community composition. *FEMS Microbiology Ecology*, 56(3), 406–417.

Kritzberg, E. S., & Ekström, S. M. (2012). Increasing iron concentrations in surface waters—A factor behind brownification? *Biogeosciences*, 9, 1465–1478.

Kritzberg, E. S., Hasselquist, E. M., Škerlep, M., Löfgren, S., Olsson, O., Stadmark, J., Hansson, L. A., & Laudon, H. (2020). Browning of freshwaters: Consequences to ecosystem services, underlying drivers, and potential mitigation measures. *Ambio*, 49, 375–390.

Li, H., Li, L., Yu, L., Yang, X., Shi, X., Wang, J., Li, J., & Lin, S. (2021). Transcriptome profiling reveals versatile dissolved organic nitrogen utilization, mixotrophy, and N conservation in the dinoflagellate Prorocentrum shikokuense under N deficiency. *The Science of the Total Environment*, 763, 143013.

Lie, A. A., Liu, Z., Terrado, R., Tatters, A., Heidelberg, K., & Caron, D. (2017). Effect of light and prey availability on gene expression of the mixotrophic chrysophyte, *Ochromonas* sp. *BMC Genomics*, 18, 163.

Liu, Z., Campbell, V., Heidelberg, K., & Caron, D. (2016). Gene expression characterizes different nutritional strategies among three mixotrophic protists. *FEMS Microbiology Ecology*, 92, 7.

Love, M. I., Huber, W., & Anders, S. (2014). Moderated estimation of fold change and dispersion for RNA-seq data with DESeq2. *Genome Biology*, 15, 550.

Maranger, R. P., & Pullin, M. J. (2003). Elemental complexation by dissolved organic matter in lakes: Implications for Fe speciation and the bioavailability of Fe and P. In J. H. Throp (Ed.), *Aquatic ecosystems: Interactivity of dissolved organic matter* (pp. 185–214). Academic Press, Elsevier Science.

Martin-Creuzburg, D., Sperfeld, E., & Wacker, A. (2009). Co-limitation of a freshwater herbivore by sterols and polyunsaturated fatty acids. *Proceedings of the Royal Society of London B: Biological Sciences*, 276, 1805–1814.

McKie-Krisberg, Z. M., Sanders, R. W., & Gast, R. J. (2018). Evaluation of mixotrophy-associated gene expression in two species of polar marine algae. *Frontiers in Marine Science*, 5, 273.

Oksanen, J., Blanchet, F.G., Friendly, M., Kindt, R., Legendre, P., McGlinn, D., Wagner, H. (2018). VEGAN: Community Ecology Package R package version 2.5-3. https://CRAN.R-project.org/package=vegan

Parrish, C. C. (2009). Essential fatty acids in aquatic food webs. In M. T. Arts, M. T. Brett, & M. Kainz (Eds.), *Lipids in aquatic systems* (pp. 309–326). Springer.

Peltomaa, E., & Taipale, S. (2020). Osmotrophic glucose and leucine assimilation and its impact on EPA and DHA content in algae. *PeerJ*, 8, e8363.

Peltomaa, E., Aalto, S., Vuorio, K., & Taipale, S. (2017). The importance of phytoplankton biomolecule availability for secondary production. *Frontiers in Ecology and Evolution*, 5, 128.

Phillips, D. L., & Gregg, J. W. (2001). Uncertainty in source partitioning using stable isotopes. *Oecologia*, 127, 171–179.

Piepho, M., Martin-Creuzburg, D., & Wacker, A. (2010). Simultaneous effects of light intensity and phosphorus supply on the sterol content of phytoplankton. *PLoS One*, 5(12), e15828.

Pinkart, H. G., Ringelberg, D. B., Piceno, Y. M., MacNaughton, S. J., & White, D. C. (2002). Biochemical approaches to biomass measurements and community structure. In C. J. Hurst, R. L. Crawford, G. R. Knudsen, M. J. McInerney, & L. D. Stetzenbach (Eds.), *Manual of environmental microbiology* (2nd ed., pp. 101–113). American Society for Microbiology Press.

Qualls, R. G., & Richardson, C. J. (2003). Factors controlling concentration, export, and decomposition of dissolved organic nutrients in the Everglades of Florida. *Biogeochemistry*, 62, 197–229.

Raven, J. A. (1995). Comparative aspects of chrysophyte nutrition with emphasis on carbon, phosphorus and nitrogen. In C. D. Sandgren, J. P. Smol, & J. Kristiansen (Eds.), *Chrysophyte algae: Ecology, phylogeny and development* (pp. 95–118). Cambridge University Press.

Raven, J. A. (1997). Phagotrophy in phototrophs. *Limnology and Oceanography*, 42, 198–205.

Roth, M. S., Gallaher, S. D., Westcott, D. J., Iwai, M., Louie, K. B., Mueller, M., Walter, A., Foflonker, F., Bowen, B. P., Ataii, N. N., Song, J., Chen, J. H., Blaby-Haas, C. E., Larabell, C., Auer, M., Northen, T. R., Merchant, S. S., & Niyogi, K. K. (2019). Regulation of oxygenic photosynthesis during trophic transitions in the green alga *Chromochloris zofingiensis*. *Plant Cell*, *31*(3), 579–601.

Ruosteenoja, K., Jylhä, K., & Kämäräinen, M. (2016). Climate projections for Finland under the RCP forcing scenarios. *Geophysica*, *51*, 17–50.

Sargent, J. R., Bell, J. G., Hendersen, R. J., & Tocher, D. R. (1995). Requirement criteria for essential fatty acids. *Journal of Applied Ichthyology*, *11*, 183–198.

Settembre, C., Fraldi, A., Medina, D. L., & Ballabio, A. (2013). Signals from the lysosome: A control Centre for cellular clearance and energy metabolism. *Nature Reviews. Molecular Cell Biology*, *14*, 283–296.

Simao, F., Waterhouse, R., Ioannidis, P., Kriventseva, E., & Zdobnov, E. (2015). BUSCO: Assessing genome assembly and annotation completeness with single-copy orthologs. *Bioinformatics*, *31*, 3210–3212.

Smith, R., Bangert, K., Wilkinson, S., & Gilmour, D. (2015). Synergistic carbon metabolism in a fast growing mixotrophic freshwater microalgal species *Micractinium inermum*. *Biomass and Bioenergy*, *8*, 73–86.

Spilling, K., Asmala, E., Haavisto, N., Haraguchi, L., Kraft, K., Lehto, A. M., Lewandowska, A., Norkko, J., Piiparinen, J., Seppälä, J., Vanharanta, M., Vehmaa, A., Ylöstalo, P., & Tamminen, T. (2022). Brownification affects phytoplankton community composition but not primary productivity in eutrophic coastal waters: A mesocosm experiment in the Baltic Sea. *Science of the Total Environment*, *841*, 156510.

Stevčić, Č., Pulkkinen, K., & Pirhonen, J. (2019). Screening of microalgae and LED grow light spectra for effective removal of dissolved nutrients from cold-water recirculating aquaculture system (RAS) wastewater. *Algal Research*, *44*, 101681.

Taipale, S. J., Vuorio, K., Strandberg, U., Kahilainen, K. K., Järvinen, M., Hiltunen, M., Peltomaa, E., & Kankaala, P. (2016). Lake eutrophication and brownification downgrade availability and transfer of essential fatty acids for human consumption. *Environment International*, *96*, 156–166.

Thrane, J. E., Hessen, D. O., & Andersen, T. (2014). The absorption of light in lakes: Negative impact of dissolved organic carbon on primary productivity. *Ecosystems*, *17*, 1040–1052.

Wilken, S., Schuurmans, J. M., & Matthijs, H. C. (2014). Do mixotrophs grow as photoheterotrophs? Photophysiological acclimation of the chrysophyte *Ochromonas danica* after feeding. *New Phytologist*, *204*(4), 882–889.

Wilken, S., Soares, M., Urrutia-Cordero, P., Ratcovich, J., Ekvall, M. K., Van Donk, E., & Hansson, L. A. (2018). Primary producers or consumers? Increasing phytoplankton bacterivory along a gradient of lake warming and browning. *Limnology and Oceanography*, *63*, S142–S155.

Zhang, Z., Sun, D., Cheng, K. W., & Chen, F. (2021). Investigation of carbon and energy metabolic mechanism of mixotrophy in *Chromochloris zofingiensis*. *Biotechnology for Biofuels*, *14*, 36.

SUPPORTING INFORMATION

Additional supporting information can be found online in the Supporting Information section at the end of this article.